

Hunting for the strangeness content of the nucleon

Gunnar Bali*, Sara Collins and Andreas Schäfer

*Institut für Theoretische Physik, Universität Regensburg,
93040 Regensburg, Germany*

E-mail:

gunnar.bali@physik.uni-regensburg.de,
sara.collins@physik.uni-regensburg.de,
andreas.schaefer@physik.uni-regensburg.de

We present results for the strangeness contribution to the nucleon, $\langle N|\bar{s}s|N\rangle$ and to the spin of the nucleon, Δs . By combining several variance reduction techniques for all-to-all propagators we are able to obtain gains in terms of computer time of factors of 25–30 for the disconnected loop that is needed within the calculation of Δs , relative to the standard approach of just employing time partitioning/dilution. For $\langle N|\bar{s}s|N\rangle$, the error is dominated by the gauge noise.

*The XXVI International Symposium on Lattice Field Theory
July 14 - 19, 2008
Williamsburg, Virginia, USA*

*Speaker.

1. Introduction

Many nucleon structure observables require the calculation of disconnected quark line diagrams for which all-to-all propagator techniques are needed. Here we present first results of an ongoing project to calculate the strangeness contribution to the spin of the nucleon Δs as well as the scalar strangeness content of the nucleon $\langle N|\bar{s}s|N\rangle$, using improved stochastic methods.

The spin of the nucleon can be factorized into a quark spin contribution $\Delta\Sigma$, a quark angular momentum contribution L_q and a gluonic contribution (spin and angular momentum) ΔG :

$$\frac{1}{2} = \frac{1}{2}\Delta\Sigma + L_q + \Delta G. \quad (1.1)$$

In the naïve $SU(6)$ quark model, $\Delta\Sigma = 1$, with vanishing angular momentum and gluon contributions. In this case sea quark contributions will be absent too and therefore there will be no strangeness contribution Δs in the factorisation,

$$\Delta\Sigma = \Delta d + \Delta u + \Delta s + \dots, \quad (1.2)$$

where in our notation Δq contains both, the spin of the quarks q and of the antiquarks \bar{q} . Experimentally Δs is usually obtained by integrating the strangeness contribution to the spin structure function g_1 over momentum transfers x . The integral over the range in which data exists ($x \gtrsim 0.004$) typically agrees with zero which means that a non-zero result relies on the unprobed very small- x region and is model dependent. Recent Hermes analysis [1] yields $\Delta s = -0.085(13)(8)(9)$ at a renormalization scale $\mu^2 = 5\text{ GeV}^2$ in the \overline{MS} scheme while our (as yet unrenormalized) results suggest $|\Delta s| < 0.01$.

The scalar strangeness density is not directly accessible in experiment but plays a rôle in models of nuclear structure. It is also of phenomenological interest since, assuming that heavy flavours are strongly suppressed, the dominant coupling of the Higgs particle to the nucleon will be accompanied by this scalar matrix element.

We will first discuss our methods, then the error reduction achieved in our present lattice setup and finally we present results on the two matrix elements, before concluding.

2. Stochastic methods

We denote the lattice spacing by a and the lattice Dirac matrix by $M = \mathbb{1} - \kappa \not{D}$. Disconnected quark line contributions require all-to-all propagators M_{ji}^{-1} where the multi-index $i = (x, \alpha, a)$ runs over all colours $a = 1, 2, 3$, spinor indices $\alpha = 1, \dots, 4$ and spacetime sites $x \in V$. Note that in our particular application it is natural and sufficient to restrict x to a given timeslice. Exact methods to obtain M^{-1} are unfeasible in terms of computer time and memory since $12V$ solver applications are required. Employing stochastic methods [2], this factor can be substituted by the number of estimates $L \ll 12V$: in a first step a set of Dirac noise vectors $\{|\eta_\ell\rangle : \ell = 1, \dots, L\}$ is generated where the $12V$ complex colour-spinor-site components are filled with $(\mathbb{Z}_2 \otimes i\mathbb{Z}_2)/\sqrt{2}$ uncorrelated random numbers [3]. These have the following properties:

$$\overline{|\eta\rangle\langle\eta|}_L := \frac{1}{L} \sum_\ell |\eta_\ell\rangle\langle\eta_\ell| = \mathbb{1} + \mathcal{O}(1/\sqrt{L}), \quad \overline{|\eta|} = \mathcal{O}(1/\sqrt{L}). \quad (2.1)$$

We will also employ the short-hand notation $\overline{|\cdot\rangle\langle\cdot|} = \overline{|\cdot\rangle\langle\cdot|}_L$. We use the conjugate gradient algorithm with even/odd preconditioning to obtain the solutions $|s_\ell\rangle$ of the sparse linear problems,

$$M|s_\ell\rangle = |\eta_\ell\rangle. \quad (2.2)$$

From these one can construct an unbiased estimate of M^{-1} :

$$E(M^{-1}) := \overline{|s\rangle\langle\eta|} = M^{-1} + M^{-1} \underbrace{(\overline{|\eta\rangle\langle\eta|} - \mathbb{1})}_{\mathcal{O}(1/\sqrt{L})}. \quad (2.3)$$

Due to the difference between $E(M^{-1})$ and M^{-1} above, any fermionic observable A can only be estimated up to a stochastic error $\Delta_{\text{stoch}}A = \mathcal{O}(1/\sqrt{L})$ on a given configuration. We define the configuration average $\langle\cdot\rangle_c$ over n_{conf} uncorrelated configurations and normalize this appropriately:

$$\sigma_{A,\text{stoch}}^2 := \frac{\langle\Delta_{A,\text{stoch}}^2\rangle_c}{n_{\text{conf}}}. \quad (2.4)$$

For large L and n_{conf} this will scale like $\sigma_{A,\text{stoch}}^2 \propto (Ln_{\text{conf}})^{-1}$. We also define the gauge error $\sigma_{A,\text{gauge}}^2 \propto n_{\text{conf}}^{-1}$ as the variation of the estimates of A over gauge configurations. This will be minimized at fixed n_{conf} if A is calculated exactly. In general the gauge error is limited by,

$$\sigma_{A,\text{gauge}}^2 \geq \sigma_{A,\text{stoch}}^2. \quad (2.5)$$

If $\sigma_{A,\text{stoch}}^2 \simeq \sigma_{A,\text{gauge}}^2$ then obviously it is worthwhile to improve the quality of the estimates while if $\sigma_{A,\text{stoch}}^2 \ll \sigma_{A,\text{gauge}}^2$ then precision can only be gained by increasing n_{conf} , possibly reducing L to save computer time since the same n_{conf}^{-1} scaling enters both sides of the inequality.

In our calculation of Δs the stochastic error initially was dominant. Hence we combined several variance reduction techniques to reduce this:

- partitioning (also coined dilution) [4]: we only set $|\eta_\ell\rangle \neq 0$ on one timeslice. This removes some of the (larger) off-diagonal noise elements, see eq. (2.3), and reduces the variance.
- hopping parameter expansion (HPE) [5]: the first few terms of the hopping parameter expansion of $\text{Tr}(\Gamma M^{-1}) = \text{Tr}[\Gamma(1 - \kappa D)^{-1}]$ vanish identically but still contribute to the noise. For the Wilson action, $\text{Tr}(\Gamma M^{-1}) = \text{Tr}(\Gamma \kappa^n D^n M^{-1})$ for $n = 4, 8$, depending on Γ , where for $\Gamma = \mathbb{1}$ one can easily calculate and correct for the zero-order difference.
- truncated solver method (TSM) [6]: calculate approximate solutions $|s_{n_t,\ell}\rangle$ after n_t solver iterations (before convergence), and estimate the difference stochastically to obtain an unbiased estimate of M^{-1} :

$$E(M^{-1}) = \overline{|s_{n_t}\rangle\langle\eta|}_{L_1} + \overline{(|s\rangle - |s_{n_t}\rangle)\langle\eta|}_{L_2} \quad \text{where} \quad L_2 \ll L_1.$$

- Truncated eigenmode approach (TEA) [7, 8]: calculate the n_{ev} lowest eigenvalues and eigenvectors of $Q = \gamma_5 M = Q^\dagger$, $Q^{-1} = Q_\perp^{-1} + \sum_{i=1}^{n_{\text{ev}}} |u_i\rangle q_i^{-1} \langle u_i|$, and stochastically estimate the complement Q_\perp^{-1} (with deflation included for free).

3. Lattice setup and error reduction

Our exploratory calculations are performed on $V = 16^3 \times 32$ configurations of $n_f \approx 2 + 1$ rooted stout-link improved staggered quarks with a Symanzik improved gauge action. These were provided by the Wuppertal group. The lattice spacing is fairly coarse, $a^{-1} \approx 1.55$ GeV, and the spatial dimension is around 2 fm [9]. We used the Wilson action for our valence quarks and currents with $\kappa = 0.166, 0.1675$ and 0.1684 , corresponding to pseudoscalar masses of about 600, 450 and 300 MeV respectively. The analysis was performed on 326 configurations at $\kappa_{\text{loop}} = 0.166$, 167 configurations at $\kappa_{\text{loop}} = 0.1675$ and 152 configurations at $\kappa_{\text{loop}} = 0.1684$, where κ_{loop} refers to the κ value of the disconnected loop. Throughout we used a modified version of the Chroma code [10].

On each configuration the disconnected loop was calculated using the stochastic variance reduction techniques detailed above (the TEA was only used at $\kappa_{\text{loop}} = 0.1684$, where 20 eigenvalues were calculated). We investigate the reduction in computer time, using optimized stochastic estimates, relative to those without any improvement techniques applied (except for time partitioning). We state all costs in terms of the average *real* computer time required on a Pentium 4 PC for one solver application (unimproved estimate), where we account for all overheads of the improvement methods.

$\text{Tr}(\Gamma_{\text{loop}} M^{-1})$	κ_{loop}	cost	loop^{opt}	$\sigma_{\text{stoch}}^{\text{opt}}$	loop	σ_{stoch}
$\Gamma_{\text{loop}} = \frac{1}{3} \sum_j \gamma_j \gamma_5$	0.166	300	-0.008(50)	0.016		
		100	-0.033(55)	0.027	-0.185(148)	0.135
		50	-0.054(64)	0.039	-0.446(201)	0.186
	0.1675	300	-0.085 (87)	0.030		
		100	-0.040(101)	0.054	0.003(211)	0.198
		50	-0.038(114)	0.076	0.056(265)	0.271
	0.1684	300	-0.069(95)	0.015		
		100	-0.068(96)	0.036	-0.089(216)	0.212
$\Gamma_{\text{loop}} = \mathbb{1}$	0.166	300	14702.6(7)	0.04		
		12	14702.5(7)	0.18	14703.5 (9)	0.47
		6	14702.3(8)	0.23	14703.7(1.0)	0.65
	0.1675	300	14743.1(1.1)	0.06		
		12	14743.4(1.2)	0.33	14745.0(1.3)	0.69
		6	14743.5(1.2)	0.42	14744.6(1.5)	0.96
	0.1684	300	14764.9(1.2)	0.04		
		100	14764.9(1.2)	0.08	14764.6(1.2)	0.27

Table 1: Results for the disconnected loop, averaged over configurations, obtained with (loop^{opt}) and without (loop) variance reduction techniques. The cost is in units of the average computer time required to solve for one (undeflated) right hand side.

Results for the configuration averages of the loops $\text{Tr}(\Gamma_{\text{loop}} M^{-1})$ are given in table 1. The gauge errors σ_{gauge} (that also depend on the stochastic noise) are displayed in brackets after the loop averages. These can be compared to the purely stochastic errors σ_{stoch} , defined in eq. (2.4).

The deflation at $\kappa_{\text{loop}} = 0.1684$ where we apply TEA accelerates the solver but time is required for the eigenvector set-up. In our implementation the cost of solving for about 90 undeflated right hand sides equals that of 90 deflated ones (including this overhead). This is why in this case we do not display results obtained at the lower cost values.

For $\text{Tr}(\frac{1}{3} \sum_j \gamma_j \gamma_5 M^{-1})$ the stochastic error dominates over the gauge error unless L is chosen ridiculously large or variance reduction techniques are applied. Using these techniques the error is brought under control to the extent that we only need to invest the computer time equivalent of roughly 100 unimproved stochastic estimates to achieve $\sigma_{\text{stoch}} < \frac{1}{2} \sigma_{\text{gauge}}$. In particular, we find a reduction in σ_{stoch}^2 (which is proportional to the amount of computer time required) of approximately 25–30 for $\kappa_{\text{loop}} = 0.166$ and 0.1684. A smaller gain is obtained for the intermediate $\kappa_{\text{loop}} = 0.1675$ which may benefit from using the TEA approach. For $\text{Tr}(\mathbb{1} M^{-1})$ the situation is reversed and the gauge error clearly dominates over the stochastic error: apart from possibly the heaviest κ_{loop} there is no advantage in using variance reduction techniques.

The matrix elements,

$$\langle N, s | \bar{q} \gamma_\mu \gamma_5 q | N, s \rangle = 2M_N s_\mu \frac{\Delta q}{2} \quad (3.1)$$

and $\langle N | \bar{q} q | N \rangle$ are extracted from the ratios of three-point functions to two-point functions (at zero momentum):

$$R^{\text{dis}}(t, t_f) = -\frac{\langle \Gamma_{2\text{pt}}^{\alpha\beta} C_{2\text{pt}}^{\beta\alpha}(t_0, t_f) \sum_{\mathbf{x}} \text{Tr}(\Gamma_{\text{loop}} M^{-1}(\mathbf{x}, t; \mathbf{x}, t)) \rangle}{\langle \Gamma_{\text{unpol}}^{\alpha\beta} C_{2\text{pt}}^{\beta\alpha}(t_0, t_f) \rangle} \quad (3.2)$$

where $\Gamma_{2\text{pt}} = \Gamma_{\text{unpol}} = (1 + \gamma_4)/2$ and $\Gamma_{\text{loop}} = \mathbb{1}$ for $\langle N | \bar{q} q | N \rangle$ and $\Gamma_{2\text{pt}} = i\gamma_j \gamma_5 (1 + \gamma_4)/2$ and $\Gamma_{\text{loop}} = \gamma_j \gamma_5$ for Δq , where we average over $j = 1, 2, 3$. Note that for $q = u, d$ there is an additional connected contribution R^{con} , which we have not calculated. We combine the three κ_{loop} values with $\kappa_{2\text{pt}} = 0.166$ and 0.1675. In the limit of large times, $t_f \gg t \gg t_0$,

$$R^{\text{dis}}(t, t_f) + R^{\text{con}}(t, t_f) \rightarrow 2 \frac{\langle N, s | (\bar{q} \Gamma_{\text{loop}} q)^{\text{latt}} | N, s \rangle}{2M_N}. \quad (3.3)$$

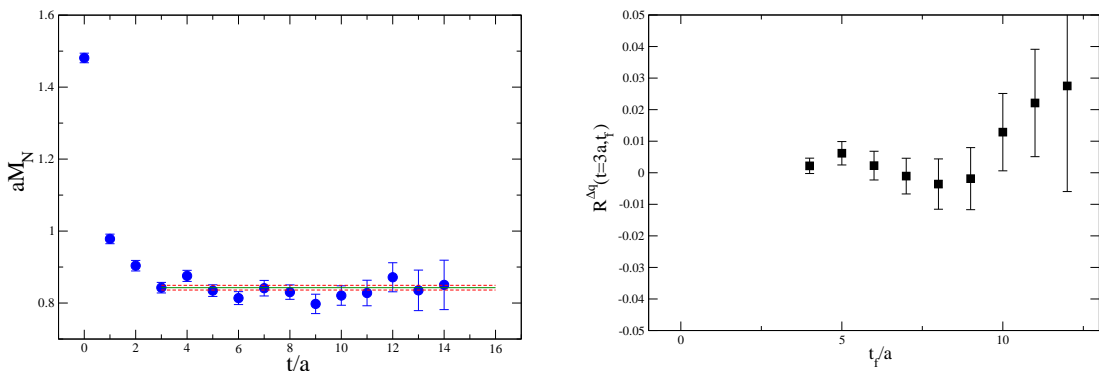


Figure 1: The effective mass of the proton with $\kappa_{2\text{pt}} = 0.166$ (left). The ratio, $R^{\Delta q}(t = 3a, t_f)$ as a function of t_f for $\kappa_{\text{loop}} = \kappa_{2\text{pt}} = 0.166$ (right).

We optimized the nucleon creation and annihilation operators using Wuppertal smearing with spatial APE-smeared parallel transporters [8]. The effective mass plot of figure 1 illustrates ground state dominance from a time $t = 3a \approx 0.38$ fm onwards. The same holds for $\kappa_{2\text{pt}} = 0.1675$. Hence

we place the source at $t_0 = 0$, the current insertion at $t = 3a$ and destroy the nucleon at $t_f \geq 4a$. The result on the right of figure 1 does not depend on t_f , even for $t_f < 6a$, indicating that indeed with the chosen temporal separations we effectively realize the large- t limit. In table 2 we display the results for Δq^{dis} at the symmetric point $t_f = 6a \approx 0.76$ fm: our methods enable us to reduce the squared errors by factors ranging from 5.5 to 11 at the fixed computational cost of 100 solver applications (in addition to calculating the two-point function). This falls somewhat short of the gains that we achieved in table 1 for the loops alone since now there are additional sources of gauge error. These we attempt to address in the near future.

	$\kappa_{\text{loop}} = 0.166$		$\kappa_{\text{loop}} = 0.1675$		$\kappa_{\text{loop}} = 0.1684$	
	$\kappa_{2\text{pt}} = 0.166$					
cost	R^{opt}	R	R^{opt}	R	R^{opt}	R
300	-0.001(4)		-0.002 (7)		-0.001 (7)	
100	-0.002(5)	+0.005(14)	-0.001 (9)	+0.008(22)	-0.004 (7)	+0.008(20)
50	+0.001(6)	+0.021(17)	+0.004(10)	+0.036(27)		
	$\kappa_{2\text{pt}} = 0.1675$					
300	-0.005(6)		-0.003(12)		-0.004(13)	
100	-0.008(7)	+0.009(23)	+0.005(15)	+0.028(35)	-0.006(13)	-0.004(28)
50	-0.002(9)	+0.046(29)	+0.023(17)	+0.083(51)		

Table 2: Results for Δq obtained with (R^{opt}) and without (R) the use of variance reduction techniques.

4. Results and Outlook

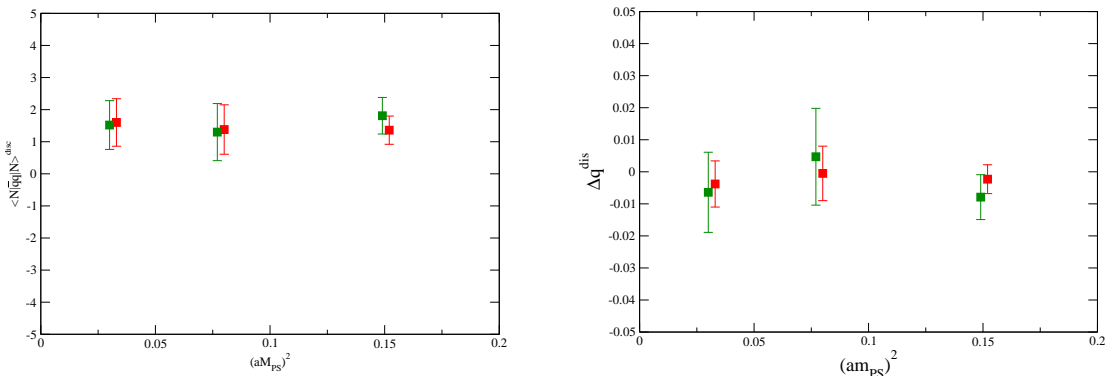


Figure 2: $\langle N | \bar{q}q | N \rangle^{\text{dis}}$ (left) and Δq^{dis} (right) as functions of the quark mass used in the disconnected loop (expressed in terms of aM_{PS}^2). The green points corresponds to a proton with $\kappa_{2\text{pt}} = 0.1675$, while for the red points $\kappa_{2\text{pt}} = 0.166$.

In figure 2 we display our results for the two matrix elements where we obtained $\langle N | \bar{q}q | N \rangle^{\text{dis}}$ at the cost of 12 solver applications per configuration and Δq^{dis} at the cost of 100 applications, in addition to the 12 applications that are necessary to calculate the two point functions. In neither case do we observe any significant dependence on the valence quark mass, varying this from $m_\pi \approx 600$ MeV down to 450 MeV, or on the loop quark mass, reducing $m_\pi \approx 600$ MeV (\simeq strange quark

mass) to $m_\pi \approx 300$ MeV. We find $|\Delta s| < 0.011$ at the heavier proton mass and $|\Delta s| < 0.022$ at the lighter mass value with 95 % confidence level while the scalar matrix element appears to be somewhat larger than one. Note however that the lattice results presented here are unrenormalized.

In the near future we will further reduce the quark masses and the statistical errors, in particular also of the scalar density, by refining our methods. We will also move to non-perturbatively improved Wilson sea quarks, allowing us to renormalize the results and to obtain a well-defined continuum limit.

Acknowledgments

We thank Z. Fodor and K. Szabo for providing us with the gauge configurations. S. Collins acknowledges support from the Claussen-Simon-Foundation (Stifterverband für die Deutsche Wissenschaft). This work was supported by the DFG Sonderforschungsbereich/Transregio 55.

References

- [1] A. Airapetian *et al.* [HERMES Collaboration], *Precise determination of the spin structure function g_1 of the proton, deuteron and neutron*, *Phys. Rev. D* **75** (2007) 012007 [[hep-ex/0609039](#)].
- [2] K. Bitar, A. D. Kennedy, R. Horsley, S. Meyer and P. Rossi, *The QCD finite temperature transition and hybrid Monte Carlo*, *Nucl. Phys. B* **313** (1989) 348.
- [3] S. J. Dong and K. F. Liu, *Stochastic estimation with $Z(2)$ noise*, *Phys. Lett. B* **328** (1994) 130 [[hep-lat/9308015](#)].
- [4] S. Bernardson, P. McCarty and C. Thron, *Monte Carlo methods for estimating linear combinations of inverse matrix entries in lattice QCD*, *Comput. Phys. Commun.* **78** (1993) 256; J. Viehoff, *News on disconnected diagrams*, *Nucl. Phys. Proc. Suppl.* **73** (1999) 856 [[hep-lat/9809073](#)]; W. Wilcox, *Noise methods for flavor singlet quantities*, [hep-lat/9911013](#).
- [5] C. Thron, S. J. Dong, K. F. Liu and H. P. Ying, *Pade-Z(2) estimator of determinants*, *Phys. Rev. D* **57** (1998) 1642 [[hep-lat/9707001](#)].
- [6] S. Collins, G. Bali and A. Schäfer, *Disconnected contributions to hadronic structure: a new method for stochastic noise reduction*, *PoS LAT2007* (2007) 141 [[0709.3217](#)].
- [7] H. Neff, N. Eicker, T. Lippert, J. W. Negele and K. Schilling, *On the low fermionic eigenmode dominance in QCD on the lattice*, *Phys. Rev. D* **64** (2001) 114509 [[hep-lat/0106016](#)]; T. A. DeGrand and S. Schäfer, *Improving meson two-point functions in lattice QCD*, *Comput. Phys. Commun.* **159** (2004) 185 [[hep-lat/0401011](#)]; L. Giusti, P. Hernandez, M. Laine, P. Weisz and H. Wittig, *Low-energy couplings of QCD from current correlators near the chiral limit*, *JHEP* **0404** (2004) 013 [[hep-lat/0402002](#)].
- [8] G. S. Bali, H. Neff, T. Düssel, T. Lippert and K. Schilling [SESAM Collaboration], *Observation of string breaking in QCD*, *Phys. Rev. D* **71** (2005) 114513 [[hep-lat/0505012](#)].
- [9] Y. Aoki, Z. Fodor, S. D. Katz and K. K. Szabo, *The equation of state in lattice QCD: with physical quark masses towards the continuum limit*, *JHEP* **0601** (2006) 089 [[hep-lat/0510084](#)].
- [10] R. G. Edwards and B. Joó, *The Chroma software system for Lattice QCD*, *Nucl. Phys. Proc. Suppl.* **140** (2005) 832 [[hep-lat/0409003](#)]; C. McClendon, *Optimized Lattice QCD kernels for a Pentium 4 cluster*, Jlab preprint (2001) JLAB-THY-01-29, http://www.jlab.org/~edwards/qcdapi/reports/dslash_p4.pdf